Real-Time Energy Management Algorithm for Plug-In Hybrid Electric Vehicle Charging Parks Involving Sustainable Energy

Ahmed Mohamed, *Member, IEEE*, Vahid Salehi, *Member, IEEE*, Tan Ma, *Graduate Student Member, IEEE*, and Osama A. Mohammed, *Fellow, IEEE*

***Abstract*—In this paper, a real-time energy management algorithm (RTEMA) for a grid-connected charging park in an industrial/commercial workplace is developed. The charging park under study involves plug-in hybrid electric vehicles (PHEVs) with different sizes and battery ratings as well as a photovoltaic (PV) system. Statistical and forecasting models were developed as components in the developed RTEMA to model the various uncertainties involved such as the PV power, the PHEVs, arrival time, and the energy available in their batteries upon their arrival. The developed energy management algorithm aims at reducing the overall daily cost of charging the PHEVs, mitigating the impact of the charging park on the main grid, and contributing to shaving the peak of the load curve. Hence, the benefits of implementing this RTEMA is shared among the customers, the charging park considering all customers as a bulk of power connected to the grid, and the ac grid. This makes it applicable for various business models. The developed RTEMA utilizes a fuzzy controller to manage the random energy available in the PHEVs' batteries arriving at the charging park and their charging/discharging times, power sharing among individual PHEVs that is commonly known as vehicle-to-vehicle functionality, and vehicle-to-grid service between the charging park and the main ac grid. The developed RTEMA was simulated using the standard IEEE 69-bus system at different penetration and distribution levels. The obtained results verify the effectiveness and validity of the developed RTEMA.**

***Index Terms*—Charging cost minimization, charging park, fuzzy, industrial/commercial zone, photovoltaic system, real-time energy management, system loading, voltage stability.**

I. Introduction

PLUG-IN hybrid electric vehicles (PHEVs) and plug-in electric vehicles (EVs) are gaining much popularity due to the global call for clean energy. Several pioneer automation companies are in the process of making PHEVs, a better option for vehicle buyers. Therefore, it is almost certain that the penetration level of these PHEVs into our national grid will keep growing.

However, the grid, in its current status, is not fully prepared yet for a high PHEV penetration level. There are some problems related to their charging process; the process of charging a random number of batteries with random energy demand represents a demand side management dilemma. For instance, it is expected that, since PHEV owners within the same society are very likely to share the general outlines of their life styles, the grid will be subjected to a big demand from PHEVs batteries at the same time when people are back from work. Therefore, researchers have developed some ideas and algorithms to manage this process [1]–[8]. The output charging rate setting of each PHEV according to these algorithms is constant during the charging period. In this paper, an RTEMA that is based on a set of priority levels of the PHEVs is developed. PHEVs will be moved from one priority level to another, and hence treated differently, based on their state of charge (SoC) and time remaining for their departure time. Moreover, previously developed algorithms did not consider the inclusion of renewable energy sources in the system, which holds the implementation of these algorithms back since we know that the concept of PHEVs is attached with obtaining the power to charge them from renewable energy. Otherwise, we end up burning more fossil fuels and hence polluting the environment even more. Saber *et al.* discerned this drawback and directed their work toward systems that involve renewable energy sources considering the added complexity and uncertainty involved with them in [9] and [10]. They aimed at minimizing the cost and emission attached with the charging process of PHEVs distributed in the network. In this paper, the energy management of a large number of PHEVs connected to the grid at the same point as a smart park [11] is developed. The main contributions of this paper are as follows:

1) to develop statistical probability density distributions for the uncertain variables involved;
2) to develop an energy management algorithm for a grid-connected charging park;
3) to involve a photovoltaic (PV) system as a renewable energy source in the developed algorithm;
4) to vary the charging rates of the EVs dynamically in real time according to their SoC.

The paper is organized as follows: in Section II, an insight of the charging park power system architecture is given; in Section III, the statistical and mathematical modeling process of the various uncertain quantities involved within the algorithm is presented; in Section IV, the developed RTEMA is presented; in Section V, some of the results obtained to verify the validity of the developed RTEMA are presented; and finally in Section VI, a summary of the conclusions that can be derived from this paper is presented.

Manuscript received May 31, 2012; revised March 07, 2013; accepted July 21, 2013. Date of publication September 30, 2013; date of current version March 18, 2014. This work was supported in part by grants from the Office of Naval Research and the U.S. Department of Energy.

A. Mohamed is with the Electrical Engineering Department, Grove School of Engineering, City College of the City University of New York, New York, NY 10031 USA (e-mail: amohamed@ccny.cuny.edu).

V. Salehi, T. Ma, and O. A. Mohammed are with the Energy Systems Research Laboratory, Florida International University, Miami, FL 33174 USA (e-mail: mohammed@fiu.edu).

Color versions of one or more of the figures in this paper are available online at http://ieeexplore.ieee.org.

Digital Object Identifier 10.1109/TSTE.2013.2278544

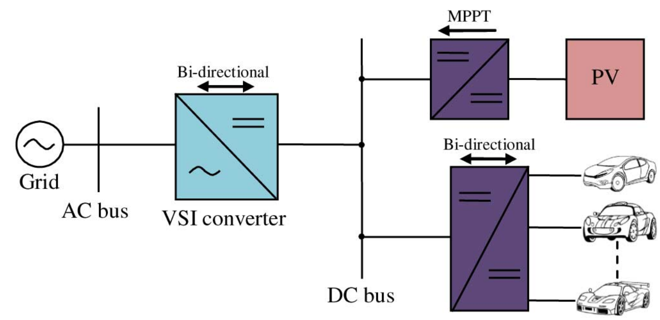

Fig. 1. One-line diagram showing a lumped model of the PHEVs charging park power system.

II. Charging Park Architecture

A one-line diagram of the system under study is shown in Fig. 1. It consists of a grid-connected charging park involving a PV system with a total capacity of 500 kW, whose maximum power point is continuously tracked and integrated into the dc-bus linking the PHEVs' batteries to the main grid. Hence, the charging park appears as a dc microgrid with local generation from the PV system and a storage system representing the PHEVs' batteries. The charging park is connected to the main grid through a bi-directional converter. The bi-directional converter is a fully controlled ac–dc/dc–ac voltage source inverter that has the capability of controlling the amount of power flowing between the ac and dc grid in both directions. Hence, the amount of power flowing in either direction can be set to a certain pre-set value, which is decided by the developed RTEMA [12].

III. Modeling System Uncertainties

The developed smart charging park is a parking garage in a workplace, possibly a university campus, which contains 1500 parking spaces. We assume that 60% of the 1500 cars parking daily in this charging park, i.e., 900 cars, are PHEVs. These 900 PHEVs are the ones managed in this study. Among the 900 PHEVs considered, around 32.5% are compact sedans with an energy consumption of 0.3 kWh/mi, 37.5% are mid-size sedans with an energy consumption of 0.45 kWh/mi, 20% are mid-size SUVs or pickups with an energy consumption of 0.6 kWh/mi, and 10% are full-size SUVs or pickups with an energy consumption of 0.75 kWh/mi.

It can be noticed that the smart charging operation involves several uncertain quantities such as the power available from the PV system, the arrival and departure times of the PHEVs, and their initial SoC when they arrive at the charging park. These quantities, despite their randomness, are crucial parameters when the energy within this system is to be managed and controlled. Therefore, various models have been developed as an attempt to model these uncertain quantities using regression techniques based on historical data or statistical techniques based on probability distribution, or density, functions (pdfs). The developed predictive models will be used for the decision-making process of the RTEMA.

A. Online PV Modeling

Since the power available from the PV system plays an essential role in the decision-making process of the developed energy management algorithm, an online forecasting model is regenerated from [13]. This model is based on statistical smoothing techniques and quantile regression. In this model, the clear sky model approach is first used to normalize the solar power. Then, adaptive linear time series models are applied for online prediction. We count on real data forecasting of PV output power. The data forecasting process was based on PV data collected over 15 years on an hourly basis, for example, the PV system in the state of Texas. The power data was set as output data to be forecasted, whereas the day of the year (1–365) and the hour of the day (1–24) were used as inputs.

TABLE I
Parameters of the Duration Time Probability Distribution

Time parameter	Arrival		Departure	
	Weekday	Weekend	Weekday	Weekend
μ_T (h)	9	11	18	15
$(\sigma_T)^2$ (h)	1.2	1.5	1.2	1.5

B. PHEVs Arrival and Departure Times

The estimated power demanded by a PHEV ($\hat{p}_{\mathrm{PHEV},i}$) can be represented by

$$\hat{P}_{\mathrm{PHEV},i} = \frac{\hat{M}_d \times E_m}{\hat{D}_t - \hat{A}_t} \tag{1}$$

where $\hat{P}_{\mathrm{PHEV},i}$ is the estimated power demanded by the ith PHEV, $\hat{M}_d$ is the estimated number of miles driven daily, E_m is the energy consumption per mile for the PHEV, $\hat{D}_t$ is the estimated departure time, and $\hat{A}_t$ is the estimated arrival time.

However, there are bounds for the values obtained from (1). In order to extend the lifetime of the batteries, upper and lower limits for their SoC are enforced. In this work, the lower limit of SoC (SoC_L) is set to 10%, which is enforced inside the PHEV itself during its operation, whereas the upper limit (SoC_U) is set to around 80%. The upper limit is enforced in the charging park. The developed algorithm will be responsible for charging the batteries of the PHEVs connected to the charging park up to that upper limit. Hence, the estimated energy needed by a PHEV for a coming day ($\hat{M}_d \times E_m$) will be set to a maximum saturation point at 70% of the total battery capacity.

In this work, the charging park is located in a place that is active from 9:00 a.m. to 6:00 p.m. Inspecting a large number, around 30 000 samples, of random PHEVs arrival and departure times, a probability distribution trend can be envisioned. Based on the central limit theorem, stating that the conditions under which the mean of a sufficiently large number of independent random variables, each with finite mean and variance, will be approximately normally distributed, the parameters of the distribution are given in Table I.

Combining the pdfs of A_t and D_t, the joint pdf of $D_t - A_t$ can be found, which is the daily parking duration. It is a normally distributed random variable with $\mu_d = 9.0$ and $\sigma_d = 1.92$. The pdf of the daily parking duration time is shown in Fig. 2.

According to [14], the average yearly total miles driven in the USA is 12 000 miles with 50% of drivers driving 25 miles/day or less, and 80% of drivers driving 40 miles or less. Therefore, a

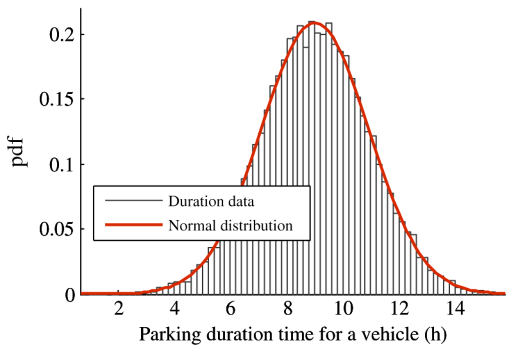

Fig. 2. PDF of the parking duration time of PHEVs ($D_t - t_A$).

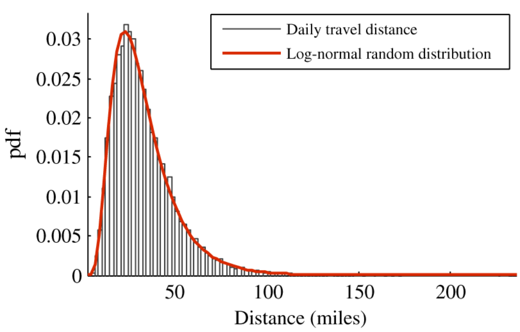

Fig. 3. PDF of the miles driven daily for PHEVs.

log-normal distribution is utilized to approximate the pdf of M_d. The results show that the total yearly driving distance average is 12 018 miles, where 48% of the vehicles drive 25 miles or less each day, and 83% of the vehicles drive 45 miles or less each day. These results, shown in Fig. 3, closely approximate the actual driving distance statistics in [14]. The distribution is then represented by

$$f_{M_d}(M_d, \mu_m, \sigma_m) = \frac{\lambda_p}{M_d \sigma_m \sqrt{2\pi}} \exp\left\{-\frac{[\ln(M_d) - \mu_m]^2}{2{\sigma_m}^2}\right\} \quad (2)$$

where $\mu_m = 3.37$ and $\sigma_m = 0.5$.

C. PHEVs Energy Demand

Using the pdf of the daily duration time, the pdf of the daily travel distance, and the power consumption of each class of the PHEVs, the pdf of the power needed by each PHEV when it is connected to the parking lot is finally found as an inverse Gaussian distribution with $\mu_p = 1.573$ and $\sigma_p = 3.652$, as shown in Fig. 4

$$f_{P_{\text{PHEV},i}}(P_{\text{PHEV},i}, \mu_p, \lambda_p) = \sqrt{\frac{\lambda_p}{2\pi {P_{\text{PHEV},i}}^3}} \exp\left\{-\frac{\lambda_p}{2{\mu_p}^2 P_{\text{PHEV},i}}(P_{\text{PHEV},i} - \mu_p)^2\right\}. \quad (3)$$

The mean value of this distribution for a given day will be used to estimate the power needed by PHEVs. At a certain time t, the total power needed by the PHEVs which will arrive during the current sample is calculated as follows:

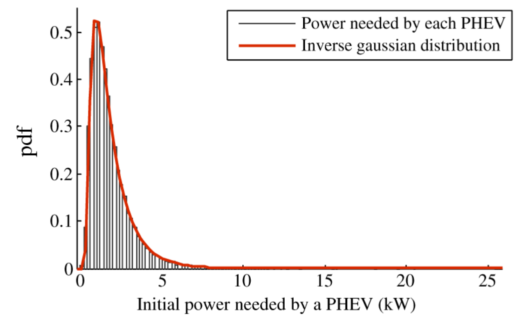

Fig. 4. PDF of the daily power needed by PHEVs.

$$\hat{P}_{\text{PHEV}} = \int_t^{t+T} f_{A_t}(t, \mu_{A_t}, \sigma_{A_t}) dt \times N \times \overline{f_{P_{\text{PHEV},i}}}. \quad (4)$$

This model, along with the forecasting model of the power generated by the PV, the hourly price of the utility grid energy, and the daily load curve, will be used to develop our RTEMA.

IV. Real-Time Energy Management Algorithm

A. PHEVs Charging Priority Levels

The charging process of the PHEVs is handled such that its impacts on the utility grid are mitigated and the overall cost of energy consumed by the PHEVs is reduced. The developed RTEMA will tend to vary the charging rates of the connected PHEVs in order to achieve these goals. The charging priority of these PHEVs is carefully considered so that we get the capability of managing the energy in the system without affecting the constraint of having all the PHEVs leaving with the desired SoC. The priority level of a PHEV is determined based on its demanded power assuming that it will be charged from its initial SoC when it arrives to the charging park to the maximum SoC desired at the same power decrement

$$P_{\text{PHEV},i} = \frac{\text{BC} \times (\text{SoC}_\text{U} - \text{SoC})}{D_t - t} \quad (5)$$

where $P_{\text{PHEV},i}$ is the power demanded by the ith PHEV. Moreover, the total power is given by

$$P_{\text{PHEV}} = \sum_{i=1}^{N} P_{\text{PHEV},i}. \quad (6)$$

The charging rates of different PHEVs with different SoCs and power requirement and correspondingly different priority levels will be handled differently. For instance, a PHEV that is connected to the parking park at 9:00 A.M., its departure time is set by the consumer to 6:00 P.M., with an SoC of 65% which is relatively high, will be charged at a relatively small charging rate. On the other hand, a PHEV that is connected to the charging park also at 9:00 A.M. but leaving at 10:30 A.M. with an SoC that is only 10% will be probably set by the RTEMA to be charged at the maximum charging rate. This is the role of the priority levels in the algorithm. Moreover, since the first car is staying for 8 h, its battery can be used as an energy storage facility for vehicle-to-vehicle (V2V) or

TABLE II
CHARGING RATE FOR DIFFERENT CHARGING LEVELS

Priority level	Power requirement	Maximum charging rate (kW)	Minimum charging rate (kW)
Level 1	$P_{\mathrm{PHEV},i} \geq 15$ kW	12	12
Level 2	10 kW < $P_{\mathrm{PHEV},i}$ < 15 kW	12	6
Level 3	5 kW < $P_{\mathrm{PHEV},i}$ < 10 kW	8	0
Level 4	2 kW < $P_{\mathrm{PHEV},i}$ < 5 kW	5	–5
Level 5	$P_{\mathrm{PHEV},i} \leq 2$ kW	2	–8

vehicle-to-grid (V2G) service. Furthermore, the charging priority of a PHEV is dynamically changing during its existence in the charging park, i.e., a PHEV may jump from a certain priority level to a higher one right before its departure. On the contrary, at a certain time if the energy price is below the daily average price and the generated PV power is more than the total power required by the PHEVs, then the extra power can be saved in some existing PHEVs and hence the priority level of these PHEVs will consequently decrease. The charging priority is shown in Table II. PHEVs in levels 1, 2, and 3 can only be charged because they need much energy either because their SoC is low, e.g., close to 10% when connected to the parking station, or their departure time is approaching but the desired SoC have not been met yet. PHEVs in levels 4 and 5 can be discharged to fulfill the V2G and V2V service. However, the PHEVs in low priority levels may jump to higher ones and vice versa as stated earlier.

B. Fuzzy Agent

A fuzzy agent will be responsible for yielding the charging rate of each PHEV ($P_{\mathrm{batt},i}$) based on the current and estimated power needed by the PHEVs, the estimated power generated by the PV, and the daily energy tariff. Without V2V and V2G service, the power flow for the current sample between the utility ac grid and the charging park can be calculated as

$$\hat{p}_{\mathrm{V2G}} = \hat{p}_{pv} - p_{\mathrm{PHEV}} - \hat{p}_{\mathrm{PHEV}}. \tag{7}$$

$\hat{p}_{\mathrm{V2G}}$ along with the energy tariff (*Tar*) will be used as the inputs for the real-time Mamdani-type [15] fuzzy logic power flow controller to determine the charging index, which will finally determine the charging rates of each charging priority level. The power flow between the utility ac grid and the dc charging park will be fuzzified as negative “N,” positive small “PS,” positive medium “PM,” positive “P,” and positive big “PB.” Similarly, the energy price will be described as very cheap “VC,” cheap “C,” normal “N,” expensive “E,” and very expensive “VE”. The method implemented for defuzzification is the centroid-based method. Within the model, minimum and maximum are used for AND and OR operators, respectively. The output of the fuzzy controller is the charging index (δ_P), which is used for adjusting the charging rates for PHEVs in different priority levels. The parameter can be described as “NB,” “N,” “Z,” “P,” and “PB,” which stand for negative big, negative, zero, positive, and positive big, respectively. The Mamdani-type model-based fuzzy rules of the fuzzy logical power flow controller are given in Fig. 5 and Table III.

The membership functions of $\hat{p}_{\mathrm{V2G}}$, *Tar*, δ_p, and the surface of the rules are shown in Fig. 5.

After gaining the charging index δ_P, which varies from $[-1 \quad 1]$, the charging rates of each charging priority levels can be calculated as follows:

$$P_{\mathrm{batt},i} = \begin{cases} 12, & \text{for level 1} \\ 9 + 3 \times \delta_P, & \text{for level 2} \\ 4 + 4 \times \delta_P, & \text{for level 3} \\ 0 + 5 \times \delta_P, & \text{for level 4} \\ \text{-3} + 5 \times \delta_P, & \text{for level 5.} \end{cases} \tag{8}$$

The sign of δ_P along with the PHEV priority level indicates whether a PHEV is charging or discharging.

C. Daily Load Curve Consideration

Based on different values of δ_p, the PHEVs in different priority levels in every sample will be charged with different charging rates. In order to limit the impacts of the charging process of PHEVs to the utility ac grid even more, the charging algorithm may also take into consideration the local load curve. For example, in the winter, the daily load curve has two peaks; one takes place at around 9:00 AM and the other at around 9:00 P.M. Moreover, the load is almost minimum at around 3:00 P.M., so it is the best time to charge the PHEVs if we want to decrease the impacts of the PHEVs to the utility ac grid.

Hence, another index σ_P will be used to adjust the power flow between the ac grid and the hybrid parking system. This index is designed based on the load curve at the main feeder. When the load demand is relatively low, below 60 kW in our design, we do not need to consider the local load and the charging rate will be just dependent on δ_P, which is the output of the fuzzy controller depending on the PHEVs demand and the energy tariff. If the load demand is between 60 and 80 kW, δ_P will be decreasing linearly from 1 to 0.9. When the load demand exceeds 80 kW, the local load is high and near the peak, so a quadratic equation with 0.9 at load 80 kW and 0 at load 100 kW will be used, which can limit the impacts from the charging parks to the ac utility grid by decreasing the charging rate. This is mathematically represented by

$$\sigma_P = \begin{cases} 1, & \overline{\hat{P}_L} \leq 0.6 \\ -0.5\overline{\hat{P}_L} + 1.3, & 0.6 < \overline{\hat{P}_L} \leq 0.8 \\ -\overline{\hat{P}_L}^2 - 2.7\overline{\hat{P}_L} + 3.7, & 0.8 < \overline{\hat{P}_L} \leq 1 \end{cases} \tag{9}$$

where $\overline{\hat{P}_L}$ is the normalized load data. After obtaining σ_P, the final charging rates for PHEVs in different priority levels can be achieved by using the following set of equations:

$$P_{\mathrm{batt},i} = \begin{cases} 12 \times \sigma_P, & \text{for level 1} \\ (9 + 3 \times \delta_P) \times \sigma_P, & \text{for level 2} \\ (4 + 4 \times \delta_P) \times \sigma_P, & \text{for level 3} \\ (0 + 5 \times \delta_P) \times \sigma_P, & \text{for level 4 if } \delta_P \geq 0 \\ (0 + 5 \times \delta_P) \times (2 - \sigma_P), & \text{for level 4 if } \delta_P < 0 \\ (-3 + 5 \times \delta_P) \times \sigma_P, & \text{for level 5 if} \delta_P \geq 0 \\ (-3 + 5 \times \delta_P) \times (2 - \sigma_P), & \text{for level 5 if } \delta_P < 0. \end{cases} \tag{10}$$

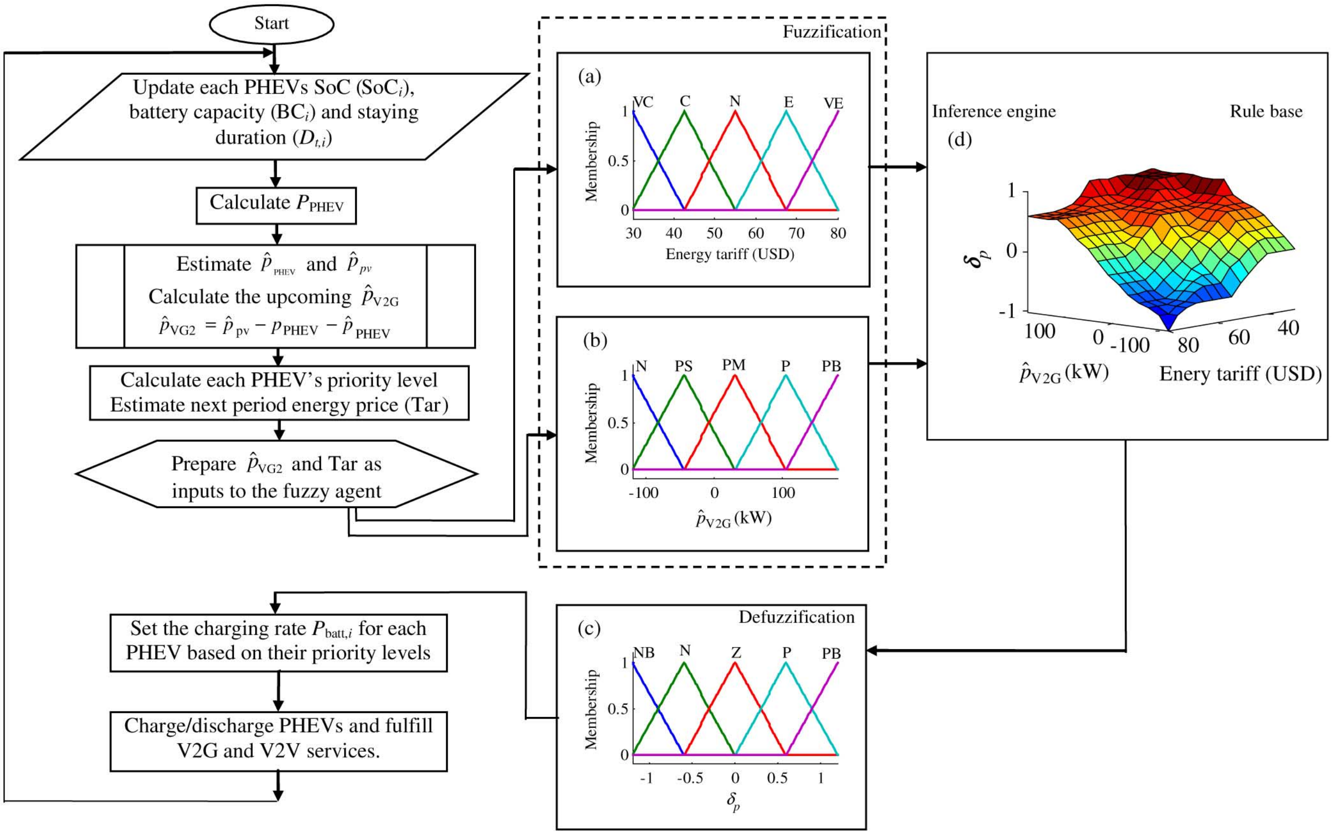

Fig. 5. Flowchart showing the developed RTEMA.

V. Results and Discussion

In order to examine the operation of the developed RTEMA, the IEEE 69-bus radial distribution system was used. Fig. 6 shows a single-line diagram of this system which includes 69 buses and 7 lateral branches. The feeder voltage is 12.66 kV and the total load in the base case is 3.82 MW and 2.85 MVar. Load flow calculations in the base case present 4.03-MW and 2.85-MVar power infeed from the external grid and a minimum voltage of 0.9 p.u. at Bus-54. The network loss is 0.23 MW or 5.7% of the total system active power. The load-flow results of the system under study are given in a table in the Appendix. All the modules of this research were implemented using two software packages linked together: the algorithm was implemented on MATLAB/SIMULINK and the output of the algorithm was transferred to DIgSILENT/PowerFactory to perform the load-flow studies. In order to study the behavior of the developed algorithm under the daily load characteristic, we defined typical daily load curves for summer and winter, which are obtained from Florida Electric Utility as shown in Fig. 7 [16]. Because the vast majority of customers in Florida are residential, peak demand in the summer season begins to climb in the morning, peaks during the hottest part of the day (4:00 P.M.), and levels off as the evening approaches. This usage pattern corresponds to the increase of loads due to air conditioning for residential customers. In the winter season, the usage pattern has two distinct peaks: a larger one (8:00 A.M.) in the mid-morning and a smaller one (8:00 P.M.) in the late evening, which correspond to residential heating loads [16]. In order to hold a consistent comparison of the cases under study, it is assumed that the normalized summer and winter curves have the same daily peak and the same daily energy consumption (kWh). Hence, we made a little change in winter curve to have the same integration as the summer curve during a 24-h day time. Therefore, the EVs daily consumption in both cases is intended to be 11.453 MWh. This amount of load is 15.5% of the total load before adding EVs (73.78 MWh). Figs. 8 and 9 show the voltage profile in all buses for 24 h. Minimum voltage of summer happens at Bus-54 at 4:12 P.M. Accordingly, the minimum voltage of winter load occurs at the same bus, but at 8:24 A.M. Fig. 10 shows the SoC of an EV during the charging process in the winter, which is connected to the grid at 8:24 A.M. Before 10:00 P.M., the output power from PV farm is not significant, and the load is in a peak period. Instead of charging the battery, this EV injects power to the grid to shave the peak of the load curve. The power injected by the EV can either supply another vehicle that needs to be charged (V2V) or be transferred to the grid (V2G); note that all the EVs are connected to the same microgrid, hence the route of the power supplied by the individual vehicles cannot be tracked. After 10:00 AM, the power

TABLE III
Fuzzy Rules

Tar\ $\hat{p}_{\text{PHEV}}$	N	PS	PM	P	PB
VC	Z	P	PB	PB	PB
C	Z	P	P	PB	PB
N	N	Z	P	P	PB
E	N	N	Z	P	P
VE	N	N	Z	P	P

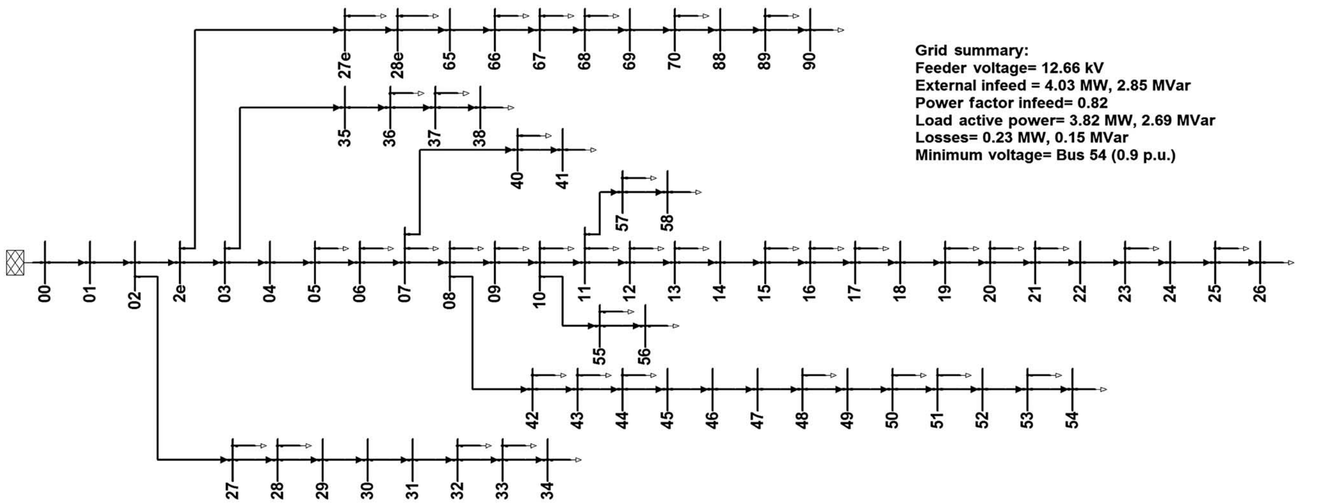

Fig. 6. 69-Bus radial distribution test feeder.

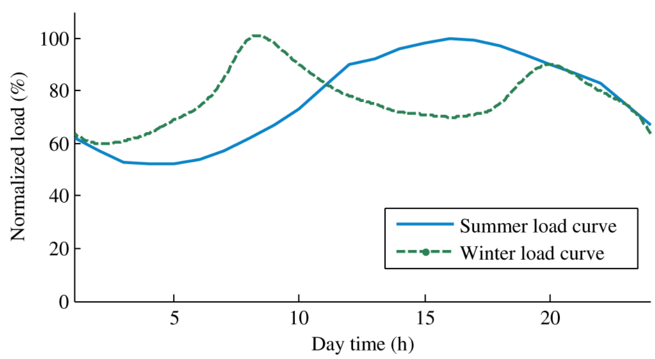

Fig. 7. Florida's normalized summer and winter daily load curves.

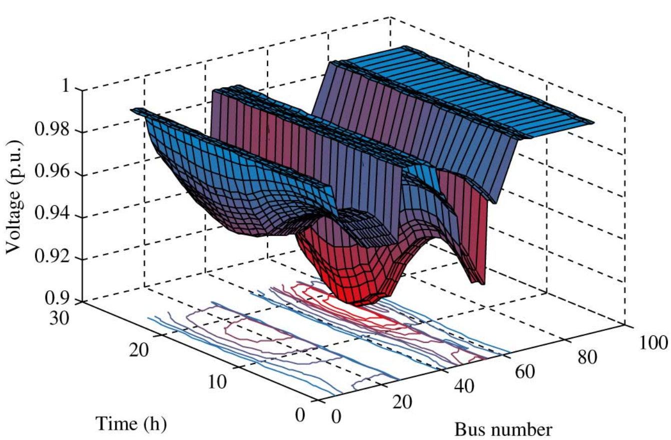

Fig. 8. 69-Bus daily voltage profile with no EVs for summer load.

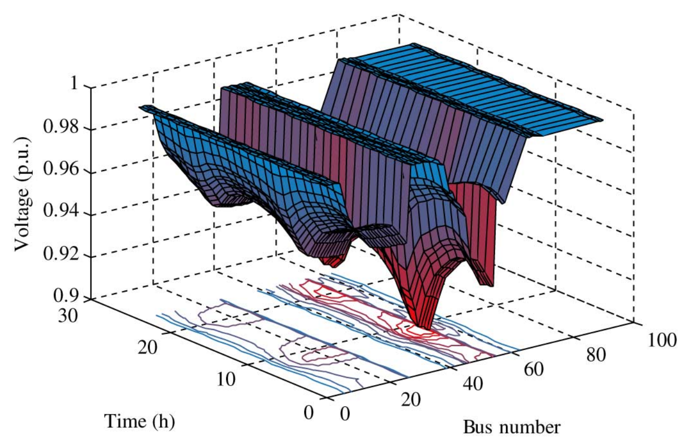

Fig. 9. 69-Bus daily voltage profile with no EVs for winter load.

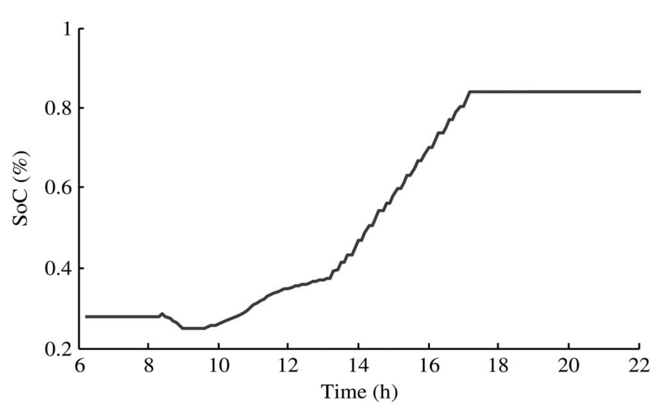

Fig. 10. SoC of an individual EV during a day as a result of implementing the developed RTEMA.

generated by the PV increases while the load decreases. The EV begins absorbing power from the grid. However, the load is still heavy. Therefore, the charging rate is small, which limits the impact of charging on the grid. After 1:00 P.M., the power generated by the PV is large, and the load is small; then it is the best time to charge the EVs, therefore the SoC of this EV increases dramatically. This process fills the valley of the load curve. The RTEMA algorithm was implemented in different cases with different techniques as follows.

A. Case A: All EVs Are Connected to Bus-20

In this case, all EVs are connected as an integrated car park to Bus-20. Without any optimization, this lumped load has the daily curve as shown in Fig. 11 with a solid line. The daily peak is 3.383 MW which occurs at 9:10 A.M. Without any energy

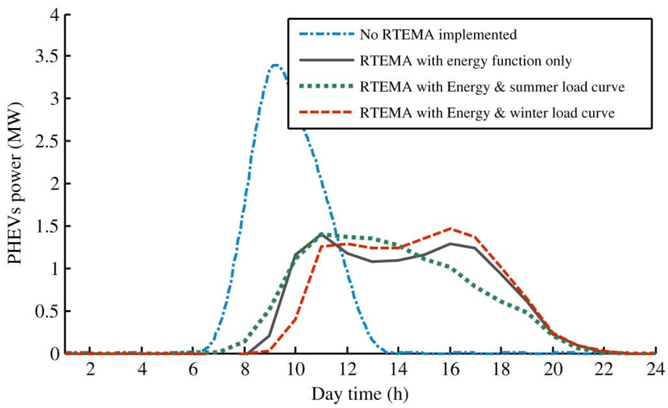

Fig. 11. PHEVs daily load profile with no optimization and different optimization objectives.

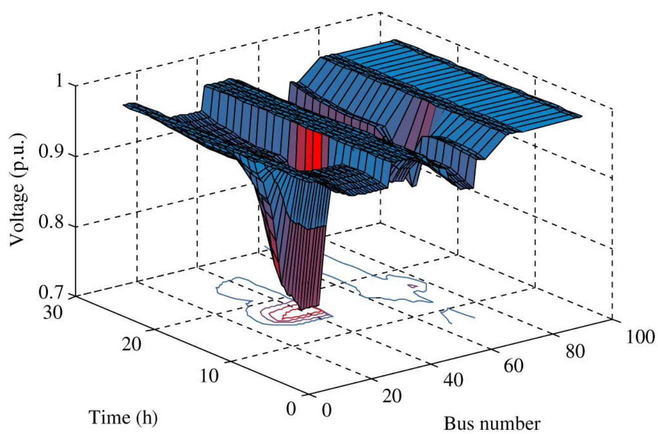

Fig. 12. Daily voltage profile with no RTEMA for summer load.

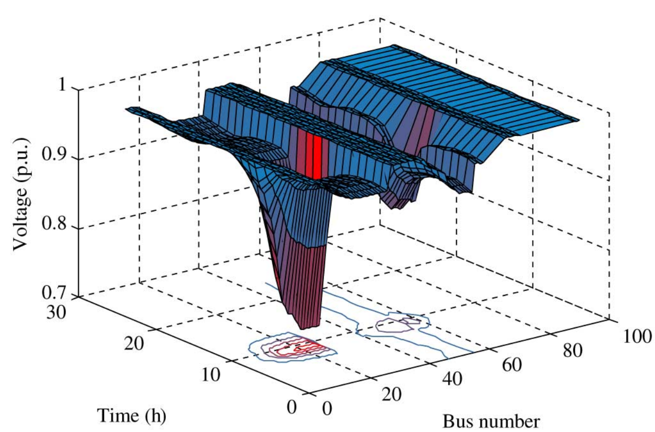

Fig. 13. Daily voltage profile with no RTEMA for winter load.

management procedure, some buses at the ends of the feeders experience high voltage drop, i.e., 0.751 p.u. with summer load and 0.72 p.u. with winter load characteristics, which are shown in Figs. 12 and 13. This drop may harm the sensitive loads on the distribution feeder and need to be improved by using the developed RTEMA. In this section, we used the optimization procedure described in Section IV. The daily active power

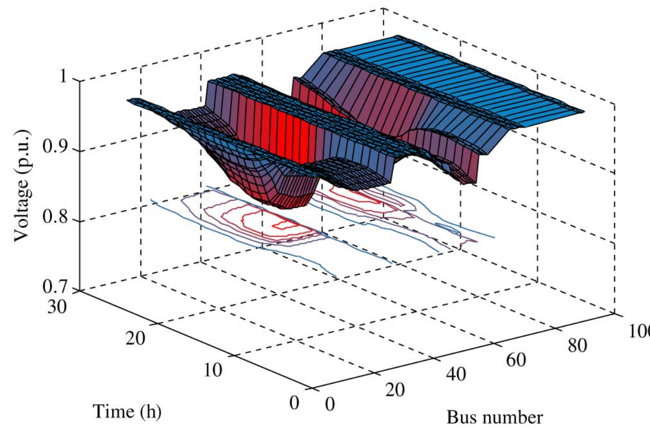

Fig. 14. Daily voltage profile with RTEMA considering energy function for summer load.

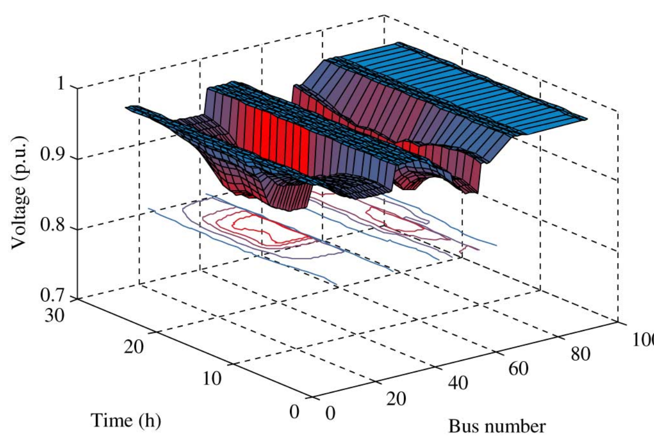

Fig. 15. Daily voltage profile with RTEMA considering energy function for winter load.

consumption of EVs is shown in Fig. 11 with a dashed–dotted curve. As can be seen, the PHEVs consumption is distributed in a long-hourly based manner and hence the peak of this load is decreased considerably and shifted to 11:00 A.M. Therefore, one of the aims of the developed algorithm, which is shaving the peak of the load curve, is achieved. The voltage daily profiles are also shown for summer and winter loads in Figs. 14 and 15, respectively, which present better voltage behavior during 24-h operation. Not only voltage is affected by using the developed RTEMA, but also the feeder losses decreased from 6.89% to 5.66% in summer and from 7.15% to 5.33% in winter load, respectively. Since the winter power losses improved more than summer losses, the results show that the performance of the RTEMA is dependent on the feeder load curves, too. Therefore, the load curves of summer and winter loads of this feeder have been included in the RTEMA as described previously. The results of the RTEMA are also demonstrated in Fig. 11 with considering summer and winter load characteristics in the energy management process. As shown in Fig. 7, the peak load of summer occurs at 4:00 P.M. Therefore, by considering the load curve, the RTEMA tries to put less loading stress around this time which is obvious in Fig. 11 with a long-dashed curve.

TABLE IV
SUMMARY OF THE RESULTS OF USING RTEMA IN 69-BUS RADIAL DISTRIBUTION FEEDER IN DIFFERENT CASES

	Without EVs		All EVs connected to one bus (connected to bus 20)						EVs distributed equally in 5-bus (connected to bus 20, 30, 41, 48, and 67)		EVs distributed equally in 10-bus (connected to bus 20, 26, 30, 34, 41, 48 54, 58, 67, and 90)	
			Not optimized		Optimized with energy		Optimized with energy and load-curve		Optimized with energy and load-curve		Optimized with energy and load-curve	
	Summer	Winter	Summer	Winter	Summer	Winter	Summer	Winter	Summer	Winter	Summer	Winter
EV's daily load (MWh)	0	0	11.453	11.453	11.584	11.584	11.395	11.551	11.395	11.551	11.395	11.551
Daily infeed (MWh)	73.787	73.786	88.001	88.370	86.988	86.808	86.724	86.815	85.766	85.835	85.841	85.901
Daily power loss (MWh)	3.308	3.196	6.068	6.327	4.924	4.634	4.85	4.674	3.892	3.694	3.967	3.761
Daily power loss (%)	4.48	4.33	6.89	7.15	5.66	5.33	5.59	5.38	4.53	4.30	4.62	4.37
Minimum voltage (p.u.)	0.9 (Bus-54) (4:12 P.M.)	0.9 (Bus-54) (8:24 A.M.)	0.751 (Bus-26) (9:12 A.M.)	0.72 (Bus-26) (9:12 A.M.)	0.877 (Bus-26) (4:12 P.M.)	0.881 (Bus-26) (10:48 A.M.)	0.879 (Bus-26) (12:36 A.M.)	0.886 (Bus-26) (4:00 P.M.)	0.891 (Bus-54) (3:48 P.M.)	0.899 (Bus-54) (8:24 A.M.)	0.888 (Bus-54) (3:48 P.M.)	0.899 (Bus-54) (8:24 A.M.)
Maximum loading (MW)	4.035 (4:12 P.M.)	4.079 (8:24 A.M.)	7.238 (9:12 A.M.)	8.636 (9:12 A.M.)	5.546 (4:12 P.M.)	5.008 (10:24 A.M.)	5.319 (2:00 P.M.)	4.754 (11:12 A.M.)	5.195 (2:00 P.M.)	4.63 (11:12 A.M.)	5.204 (2:00 P.M.)	4.638 (11:12 A.M.)
Cost (USD/day)	–	–	1314	1300	1156	1104	1156	1143	–	–	–	–

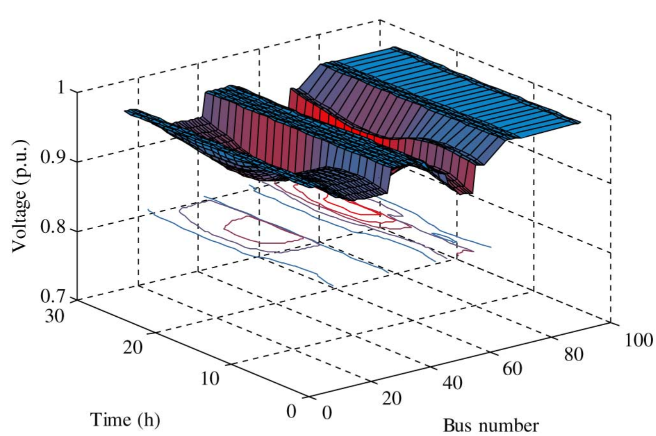

Fig. 16. Daily voltage profile with RTEMA considering energy function and summer load curve.

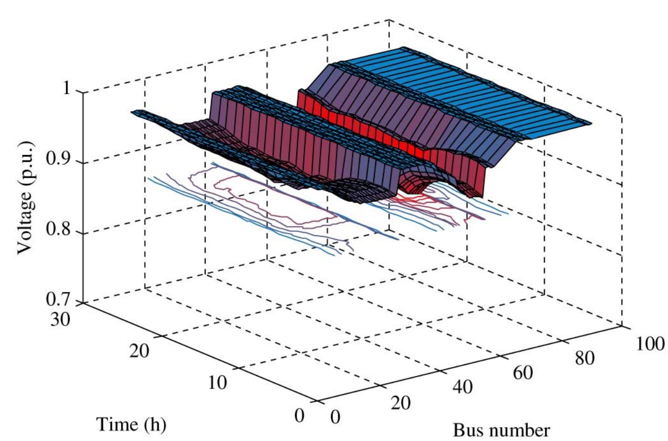

Fig. 17. Daily voltage profile with RTEMA considering energy function and winter load curve.

Accordingly, for winter load curve with two peaks, the main one at 8:00 A.M. and the minor one at 8:00 P.M., the RTMEA tends to charge the PHEVs after the first peak and before the second peak. The daily voltage profiles improved in these cases and are similar to Figs. 14 and 15. Therefore, the developed algorithm mitigates the impact of the charging park on the main grid.

B. Case B: All EVs Are Distributed Equally to Five Buses

In order to study the effect of the PHEVs load distribution in radial distribution feeder, in this case all the PHEVs are distributed equally at buses 20, 30, 41, 48, and 67. Hence, the same amount of load which was considered in the previous case is equally distributed at these nodes and the RTEMA uses the PHEVs' same daily distribution curve and feeder total daily load curve to manage the PHEVs charging process. Therefore, the results of the RTEMA are similar to the previous cases for the summer and winter optimized daily load curves. The 24-hr daily load-flow results in better voltage profiles, which are shown in Figs. 16 and 17 for summer and winter loads, respectively. The RTEMA objective function is based on energy by considering feeder load characteristics. The voltage profiles in this case are similar to feeder main profiles before connecting EVs, i.e., Figs. 8 and 9. Table IV presents a summary of the results for all cases studied in this paper. Obviously, the feeder total losses and voltage profile improved in this case, too. For example, in the summer load case, the feeder total loss is decreased from 5.59% to 4.53%.

C. Case C: All EVs Are Distributed Equally to 10 Buses

In this last case, all the PHEVs are distributed equally among 10 buses in order to study the PHEVs parking distribution effect in radial feeder. These nodes are: 20, 26, 30, 34, 41, 48, 54, 58, 67, and 90. Similar to the previous case, the RTEMA will improve the system voltage profiles. The response will be more similar to the previous case and is comparable to the case with no EVs. The results of minimum voltage, total loss of feeder, and its maximum loading and peak hours are also presented in Table IV, and they illustrate that more distribution of EVs does not have a significant effect on radial distribution system parameters anymore.

Finally, it can also be seen in Table IV that the overall cost of charging the PHEVs is reduced by a ratio that ranges from 12% to 16% using the developed RTEMA. This means that the developed algorithm succeeds in reducing the overall daily cost of charging the EVs. A future work suggested by the authors is to put this complex time-variant optimization problem in a closed formula and solve it using an optimization tool.

VI. Conclusion

In this paper, a real-time energy management algorithm for a grid-connected smart charging park based on charging priority levels was developed. The developed algorithm allows V2G and V2V functionalities and aims at minimizing the total cost of charging by handling the charging rates of the EVs. An advantage of the developed algorithm is that the charging rates of the EVs during their parking period are varying according to their state of charge. A fuzzy agent was used as a component within the developed algorithm. Energy tariff, load demand, and PV output power profiles are elements within the algorithm. The performance of the developed algorithm was tested by simulating it on a charging park connected to the IEEE standard 69-bus system at different penetration and distribution levels. The results show a reduction in the overall cost of charging as well as a significant improvement in the voltage profile and the losses in the system. The developed algorithm would also be beneficial to the utility grid even if the price rate is flat, because the load curve will still be shaved since the load curve is used as a factor in defining the charging rates of the vehicles. It will also be beneficial for charging park operators, although relatively less beneficial, since they still have the capability of reducing the overall cost of energy by managing the V2V service, which is independent from the energy tariff. This algorithm is easy to be developed and implemented because it is not based on an optimization technique and hence several objectives can be targeted, simultaneously. However, it may have a drawback of deviating from the optimal point.

Appendix

The load-flow results of the test system, shown in Fig. 6, are as follows:

Load-Flow Results of the Test System

Bus name	Voltage (p.u.)	Voltage angle (deg)	Voltage deviation (%)	Active power (MW)	Reactive power (KVar)
0	1.000	0.000	0.000	0.000	0.000
1	1.000	–0.001	–0.003	0.000	0.000
2	1.000	–0.002	–0.007	0.000	0.000
3	1.000	–0.004	–0.010	0.000	0.000
4	0.999	–0.016	–0.093	0.000	0.000
5	0.990	0.059	–0.994	0.003	0.002
6	0.981	0.138	–1.930	0.040	0.030
7	0.973	–0.287	–2.684	0.075	0.054
8	0.969	–0.506	–3.066	0.030	0.022
9	0.964	–0.419	–3.571	0.028	0.019
10	0.961	–0.560	–3.868	0.145	0.104
11	0.958	–0.506	–4.188	0.145	0.104
12	0.955	–0.459	–4.483	0.008	0.006
13	0.952	–0.412	–4.776	0.008	0.006
14	0.949	–0.365	–5.066	0.000	0.000
15	0.949	–0.356	–5.120	0.046	0.030
16	0.948	–0.342	–5.209	0.060	0.035
17	0.948	–0.342	–5.210	0.060	0.035
18	0.947	–0.333	–5.257	0.000	0.000
19	0.947	–0.327	–5.287	0.001	0.001
20	0.947	–0.318	–5.336	0.114	0.081
21	0.947	–0.318	–5.337	0.005	0.004
22	0.947	–0.317	–5.344	0.000	0.000
23	0.946	–0.314	–5.360	0.028	0.020
24	0.946	–0.310	–5.377	0.000	0.000
25	0.946	–0.309	–5.384	0.014	0.010
26	0.946	–0.309	–5.386	0.014	0.010
27	1.000	–0.003	–0.007	0.026	0.019
28	1.000	–0.005	–0.015	0.026	0.019
29	1.000	–0.003	–0.027	0.000	0.000
30	1.000	–0.003	–0.029	0.000	0.000
31	1.000	–0.001	–0.040	0.000	0.000
32	0.999	0.004	–0.065	0.014	0.010
33	0.999	0.009	–0.099	0.020	0.014
34	0.999	0.010	–0.105	0.006	0.004
35	1.000	–0.005	–0.015	0.000	0.000
36	0.999	–0.050	–0.140	0.079	0.056
37	0.995	–0.189	–0.524	0.385	0.275
38	0.994	–0.209	–0.578	0.385	0.275
40	0.973	–0.286	–2.687	0.041	0.028
41	0.973	–0.286	–2.688	0.004	0.003
42	0.967	–0.484	–3.348	0.004	0.004
43	0.963	–0.458	–3.675	0.026	0.019
44	0.959	–0.422	–4.127	0.024	0.017
45	0.954	–0.386	–4.568	0.000	0.000
46	0.932	0.017	–6.837	0.000	0.000
47	0.920	0.224	–7.954	0.000	0.000
48	0.916	0.306	–8.386	0.100	0.072
49	0.911	0.413	–8.893	0.000	0.000
50	0.904	0.483	–9.640	1.244	0.888
51	0.903	0.486	–9.669	0.032	0.023
52	0.903	0.489	–9.708	0.000	0.000
53	0.901	0.508	–9.900	0.227	0.162
54	0.900	0.513	–9.958	0.059	0.042
55	0.961	–0.559	–3.874	0.018	0.013
56	0.961	–0.559	–3.874	0.018	0.013
57	0.958	–0.500	–4.221	0.028	0.020
58	0.958	–0.500	–4.221	0.028	0.020
65	1.000	–0.012	–0.041	0.000	0.000
66	1.000	–0.012	–0.046	0.024	0.017
67	1.000	–0.013	–0.046	0.024	0.017
68	0.999	–0.024	–0.116	0.001	0.001
69	0.999	–0.028	–0.145	0.000	0.000
70	0.999	–0.029	–0.149	0.006	0.004
88	0.999	–0.029	–0.150	0.000	0.000
89	0.998	–0.031	–0.160	0.039	0.026
90	0.998	–0.031	–0.160	0.039	0.026

References

[1] S. Deilami, A. Masoum, P. Moses, and M. Masoum, "Real-time coordination of plug-in electric vehicle charging in smart grids to minimize power losses and improve voltage profile," *IEEE Trans. Smart Grid*, vol. 2, no. 3, pp. 456–467, Sep. 2011.

[2] E. Sortomme, M. Hindi, S. MacPherson, and S. Venkata, "Coordinated charging of plug-in hybrid electric vehicles to minimize distribution system losses," *IEEE Trans. Smart Grid*, vol. 2, no. 1, pp. 198–205, Mar. 2011.

[3] W. Di, D. Aliprantis, and Y. Lei, "Load scheduling and dispatch for aggregators of plug-in electric vehicles," *IEEE Trans. Smart Grid*, vol. 3, no. 1, pp. 368–376, Mar. 2012.

[4] W. Chenye, H. Mohsenian-Rad, and H. Jianwei, "Vehicle-to-aggregator interaction game," *IEEE Trans. Smart Grid*, vol. 3, no. 1, pp. 434–442, Mar. 2012.

[5] A. Al-Awami and E. Sortomme, "Coordinating vehicle-to-grid services with energy trading," *IEEE Trans. Smart Grid*, vol. 3, no. 1, pp. 453–462, Mar. 2012.

[6] S. Shahidinejad, S. Filizadeh, and E. Bibeau, "Profile of charging load on the grid due to plug-in vehicles," *IEEE Trans. Smart Grid*, vol. 3, no. 1, pp. 135–141, Mar. 2012.

[7] D. Tuttle and R. Baldick, "The evolution of plug-in electric vehicle-grid interactions," *IEEE Trans. Smart Grid*, vol. 3, no. 1, pp. 500–505, Mar. 2012.

[8] T. Sousa, H. Morais, Z. Vale, P. Faria, and J. Soares, "Intelligent energy resource management considering vehicle-to-grid: A simulated annealing approach," *IEEE Trans. Smart Grid*, vol. 3, no. 1, pp. 535–542, Mar. 2012.

[9] A. Saber and G. Venayagamoorthy, "Plug-in vehicles and renewable energy sources for cost and emission reductions," *IEEE Trans. Ind. Electron.*, vol. 58, no. 4, pp. 1229–1238, Apr. 2011.

[10] A. Saber and G. Venayagamoorthy, "Efficient utilization of renewable energy sources by gridable vehicles in cyber-physical energy systems," *IEEE Syst. J.*, vol. 4, no. 3, pp. 285–294, Sep. 2010.

[11] P. Mitra, G. Venayagamoorthy, and K. Corzine, "SmartPark as a virtual STATCOM," *IEEE Trans. Smart Grid*, vol. 2, no. 3, pp. 445–455, Sep. 2011.

[12] A. Mohamed, M. Elshaer, and O. Mohammed, "Bi-directional ac-dc/dc-ac converter for power sharing of hybrid ac/dc systems," in *Proc. IEEE PES General Meeting 2011*, Detroit, MI, USA, 2011.

[13] P. Bacher, H. Madsen, and H. Nielsen, "Online short-term power forecasting," *Solar Energy*, vol. 83, no. 10, pp. 1772–1783, Oct. 2009.

[14] L. Sanna, "Driving the solution the plug-in hybrid electric vehicle," *EPRI J.*, vol. 1, pp. 8–17, Fall 2005.

[15] K. M. Passino and S. Yurkovich, *Fuzzy Control*, Menlo Park, CA, USA: Addison-Wesley Longman, 1998.

[16] "Review of the 2011ten-year site plans for Florida's electric utilities," *Florida Public Service Commission*, Tallahassee, FL, USA, Nov. 2011 [Online]. Available: http://www.floridapsc.com.

Ahmed Mohamed (El-Tallawy) (S'09–M'13) was born in Minia, Egypt, in 1984. He received the B.Sc. and M.Sc. degrees from the College of Engineering, Minia University, Minia, Egypt, in 2006 and 2009, respectively. From 2009 to 2013, he was a Ph.D. candidate and a research/teaching assistant at the ESRL, Florida International University, Miami, FL, USA.

From 2006 to 2009, he was a research/teaching assistant at the College of Engineering, Minia University. He is currently an assistant professor at the Electrical Engineering Department, Grove School of Engineering, City College of New York, City University of New York. He was a post-doctoral research fellow at the Energy Systems Research Laboratory (ESRL), Florida International University. His current research interests include hybrid ac/dc power systems, pulsed loads, renewable energy systems, microgrids, and smart grids.

Vahid Salehi (S'09–M'13) was born in Tabriz, Iran, in 1980. He received the B.S. degree in electrical engineering from the University of Tabriz, Iran, in 2003, and the M.Sc. degree in power system engineering from the University of Tehran, Iran, in 2006. He is currently working toward the Ph.D. degree at Florida International University.

From 2003 to 2008, he was working with the Energy Research Institute (MATN) in Tehran, Iran. His research interests include power system studies, smart grid, renewable energy integration and energy conversion in power systems, distributed energy resource integration, dynamic modeling of power systems, power system stability, protection, wide-area monitoring, and control and protection of power systems. His dissertation related to the development and verification of control and protection strategies in wide-area power systems for smart grid applications.

Tan Ma (GS'10) was born in Xinyang, China. He received the M.Eng. degree in control theory and control engineering from Huazhong University of Science and Technology (HUST) in China, in 2009, and the B.Eng. degree in automation from HUST in China, in 2007. He is currently working toward the Ph.D. degree in the Energy Systems Research Laboratory at the Electrical and Computer Engineering Department, Florida International University, Miami, FL, USA.

His current research interests include application of intelligent control to power systems, energy storage systems, hybrid ac/dc power systems, renewable energy systems, plug-in electrical vehicles charging systems, and smart grids.

Osama A. Mohammed (S'80–M'83–SM'88–F'96) received the M.S. and Ph.D. degrees in electrical engineering from Virginia Polytechnic Institute and State University.

He is a professor of Electrical and Computer Engineering and the Director of the Energy Systems Research Laboratory at Florida International University. He published numerous journal articles over the past 30 years in areas relating to power systems, electric machines and drives, computational electromagnetics, and in design optimization of electromagnetic devices, artificial intelligence applications to energy systems. He authored and coauthored more than 300 technical papers in the archival literature. He has conducted research work for government and research laboratories in shipboard power conversion systems and integrated motor drives. He is also interested in the application communication and wide-area networks for the distributed control of smart power grids. He has been successful in obtaining a number of research contracts and grants from industries and federal government agencies for projects related to these areas. He also published several book chapters including: Chapter 8 on direct current machinery in the *Standard Handbook for Electrical Engineers*, 15th edition (New York, NY, USA: McGraw-Hill, 2007) and a book chapter titled "Optimal Design of Magnetostatic Devices: The Genetic Algorithm Approach and System Optimization Strategies," in the book *Electromagnetic Optimization by Genetic Algorithms*, (Hoboken, NJ, USA: Wiley, 1999).

Prof. Mohammed is the recipient of the IEEE PES 2010 Cyril Veinott Electromechanical Energy Conversion Award. He is also a Fellow of the Applied Computational Electromagnetic Society. He is Editor of IEEE Transactions on Energy Conversion, IEEE Transactions on Magnetics, *Power Engineering Letters*, and also an Editor of *COMPEL*. He is the past President of the Applied Computational Electromagnetic Society (ACES). He received many awards for excellence in research, teaching, and service to the profession and has delivered numerous invited lectures at scientific organizations around the world. He has been the general chair of several international conferences including ACES 2006, IEEE-CEFC 2006, IEEE-IEMDC 2009, IEEE-ISAP 1996, and COMPUMAG-1993. He has also chaired technical programs for other major international conferences including IEEE-CEFC 2010, IEEE-CEFC-2000, and the 2004 IEEE Nanoscale Devices and System Integration. He also organized and taught many short courses on power systems, electromagnetics, and intelligent systems in the USA and abroad. He has served ACES in various capacities for many years. He also serves IEEE in various boards, committees, and working groups at the national and international levels.